

Quantum energy spectra and one-dimensional quasiperiodic systems

Kazushige Machida and Mitsutaka Fujita

Department of Physics, Kyoto University, Kyoto, Japan

(Received 28 April 1986)

Statistical properties of energy spectra in one-dimensional quasiperiodic systems are studied numerically. We find three distinctive level distributions: the Poisson, inverse-power-law (IPL), and cosine-band-like behaviors in the Harper model with an incommensurate potential. These depend on whether the electronic state is localized, critical, or extended, respectively. Energy spectra of electrons on the quasiperiodic Fibonacci lattice are also characterized by the IPL irrespective of the strength of the modulation, indicating that the state is always critical.

Much attention has been focused on level distributions of quantum systems in various fields¹ ranging from nuclear physics to condensed-matter physics. It is believed that statistical properties of quantum spectra reflect sensitively the underlying physics and are especially suited for investigations of quantum chaos.² By solving analytically a special class of Schrödinger equation with an almost periodic or incommensurate potential, Grempel *et al.*³ were able to show profound relationships between the Anderson localization problem and the quantum chaos problem. For a one-dimensional Schrödinger operator with random potentials or in the Anderson model where the state is rigorously known to be localized, Molčanov⁴ proves that the level distribution of the spectrum is of the Poisson type with no level repulsion.

This work leads us to ask a natural question: What are the statistical properties of spectra for another class of the Schrödinger operators in the presence of incommensurate potentials and with quasiperiodic modulations? These problems belong to a class intermediate between completely random and periodic ones. The well-studied Harper model⁵ is such a system: $c_{n+1} + c_{n-1} + \lambda V(n\theta)c_n = Ec_n$ where $V(t) = \cos(2\pi t)$ and θ is irrational. The potential is incommensurate with the underlying lattice. It is known⁵⁻¹⁰ that the case $\lambda < 2$ ($\lambda > 2$) corresponds to the extended (localized) state and that the self-dual point⁶ $\lambda = 2$ gives the metal-insulator transition at which the state is neither extended nor localized but critical. The spectra of this system have also been investigated quite thoroughly,⁵⁻¹⁰ being absolute continuous, singular continuous, or pure point, depending on whether $\lambda < 2$, $\lambda = 2$, or $\lambda > 2$, respectively.

Here we would like to present our numerical results on the statistical properties of the energy spectra for the Harper model. The distribution $P(S)$ of the nearest-neighbor level spacings is markedly different depending upon λ , or upon whether the underlying state is localized, critical, or extended. Namely, when $\lambda > 2$ the distribution is of Poisson type and at $\lambda = 2$ we obtain a novel type of distribution characterized by an inverse power law (IPL).

We also present the results for another class of Schrödinger operators on a quasiperiodic lattice.^{7,11-13} This is a one-dimensional version of the so-called quasicrystals.^{14,15} The models are described by the tight-binding Hamiltonians in which (1) a set of the transfer in-

tegrals $\{t_n\}$, consisting of two kinds t_A and t_B , is given by the Fibonacci sequence $t_{n+1}c_{n+1} + t_n c_{n-1} = Ec_n$ (Fibonacci transfer model) and (2) a set of the site potentials $\{v_n\}$, consisting of v and $-v$, is placed by the Fibonacci sequence $c_{n+1} + c_{n-1} + v_n c_n = Ec_n$ (Fibonacci on-site model). We shall demonstrate that the IPL distribution can be found irrespective of the values of t_A/t_B and v in both models except for the periodic cases $t_A/t_B = 1$ and $v = 0$.

The method of numerical calculation is as follows: In the Harper model, approximating an irrational θ by F_{l-1}/F_l , where the Fibonacci numbers F_l are defined by $F_l = F_{l-1} + F_{l-2}$ with $F_0 = F_1 = 1$, we successively change the system size $N = F_l$ to effectively approach the irrational $1/\tau$ [note $\lim_{l \rightarrow \infty} (F_{l-1}/F_l) = 1/\tau$ where τ is the golden mean] and diagonalize the Hamiltonian matrices up to $N = 1597$ ($l = 16$) mainly under periodic boundary conditions. In the Fibonacci model the system size is varied according to the Fibonacci numbers. Thus the ratio of the two kinds of the elements tends to τ as $l \rightarrow \infty$. We examine the generation dependence on physical properties.

Figure 1 shows the value of the n th largest level spacing $G(n)$ (left-hand-side figures) and the histograms of the level-spacing distribution $P(S)$ (right-hand-side figures) for various values of λ in the Harper model. Note that a pair of these figures is complementary to each other because $P(x) \propto |dG(x)/dx|$.

In the case $\lambda = 1$ [Fig. 1(a)] where the state is extended $G(n)$ consists of the three parts; in the larger-spacing region a straight line is seen, giving rise to a power-law behavior (see later for details). The spacings around $G(n) \cong O(10^{-3})$ are characterized by a cosine function. The levels in this region are paired with almost zero spacing, forcing a large number of spacings to concentrate around $G(n) \cong O(10^{-6})$. This causes a very sharp peak at the origin in the distribution $P(S)$. These properties resemble those of a regular system under periodic boundary conditions.

In the case $\lambda = 3$ [Fig. 1(c)] where the state is localized $G(n)$ is best described by an exponential curve on which almost all data points sit (note the logarithmic scale). The dent located around 10^{-3} tends to vanish on increasing the system size. The same deviation in the larger-spacing region as in the $\lambda = 1$ case is seen. These features furnish

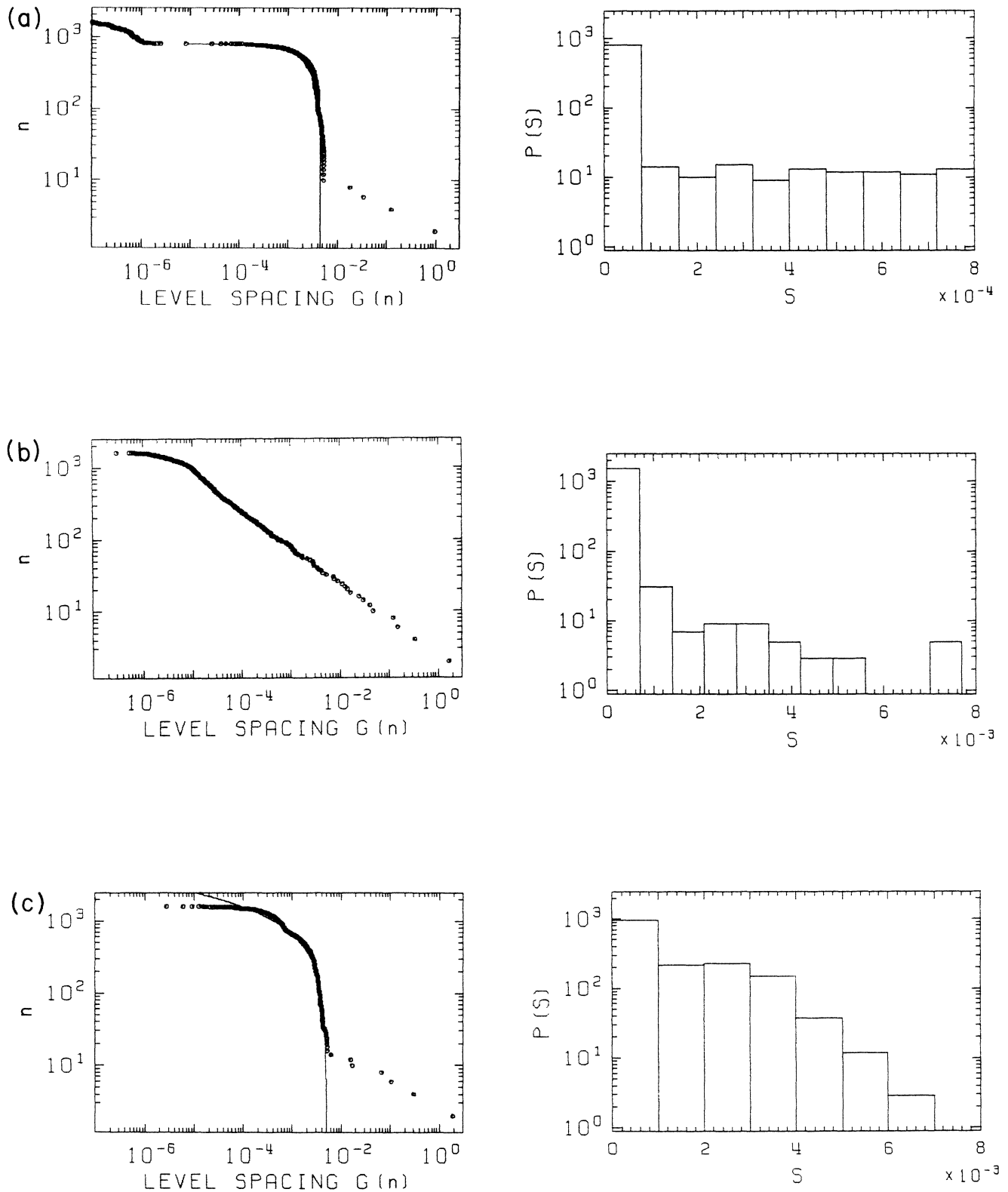


FIG. 1. Level spacings $G(n)$ arranged from the larger ones (left) and histograms of the distribution $P(S)$ (right) for the system size 1597; (a) $\lambda=1.0$ (extended case). Spacings consist of three groups: the inverse-power-law (IPL), the cosine-band-like, and the almost-zero-spacing regions (see text). Thin line is a cosine curve fitted to the data. (b) $\lambda=2$ (critical case). Straight line of $G(n)$ in this plot indicates that it obeys the IPL. $P(S)$ is also characterized by the IPL. (c) $\lambda=3$ (localized case). $G(n)$ is best described by an exponential curve (the thin line). Deviation in the larger spacing region is a remnant of the IPL. The dent around $G(n) \approx 10^{-3}$ tends to vanish as the system size is increased. $P(S)$ expressed by a straight line in this plot means the Poisson distribution.

convincing evidence that the distribution $P(S)$ is of Poisson type. Indeed the right-hand-side figure in Fig. 1(c) exhibits a Poisson distribution [$P(x) \propto e^{-x}$] which is the case in the Anderson model.⁴ Therefore both localized states in the present incommensurate potential and the random potential models show the same level-spacing distribution.

In the case $\lambda=2$ [Fig. 1(b)] where the state is critical, that is, intermediate between the extended and localized states, $G(n)$ exhibits an inverse-power-law behavior with the power index d as is unambiguously shown as a straight line in the logarithmic plot. It is evident that $P(S)$ is described by an inverse power law (IPL) distribution with the power index $d + 1$. Therefore we have obtained here the three distinctive types of the level distribution, depending upon whether the underlying states are extended, critical, or localized.

We display the results of $G(n)$ for the Fibonacci on-site model in Fig. 2. Irrespective of the values of the on-site potential v $G(n)$ is always characterized by IPL behavior with the power index or fractal dimension d which depends on v . Correspondingly, $P(S)$ is of the IPL distribution with the power $d + 1$, namely $P(x) \propto 1/x^{d+1}$ as shown in Fig. 3. These results are also true for the Fibonacci transfer model. It is interesting to note that the IPL distribution implies level attraction contrary to the level repulsion seen in the Wigner distribution^{2,3} observed in quantum chaos systems. To our knowledge there is no known example which has such an IPL distribution in the energy spectra.

In order to understand the origin of the IPL distribution, we supplement our discussion by noting the following: We have found the same branching rule for the eigenvalues in the Harper model at the self-dual point ($\lambda=2$) as in the Fibonacci model (see Ref. 13 for details). Namely the eigenvalues for system size $N = F_l$ are divided into main three subbands (see Fig. 4), each band containing exactly F_{l-2} , F_{l-3} , and F_{l-2} levels according to $F_l = F_{l-2} + F_{l-3} + F_{l-2}$. Each subband is divided into

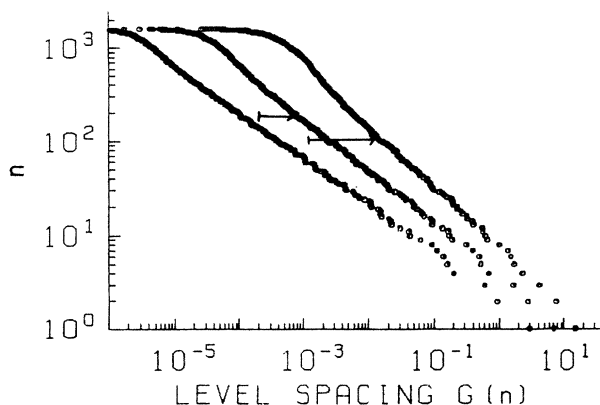


FIG. 2. Level spacing $G(n)$ in the on-site Fibonacci model for $v = 1.0, 1.4,$ and 1.8 (from the right to left) where the curves are shifted for clarity. Note that the slopes of the straight lines which are related to the power index d depend on v . (The system size is 1597.)

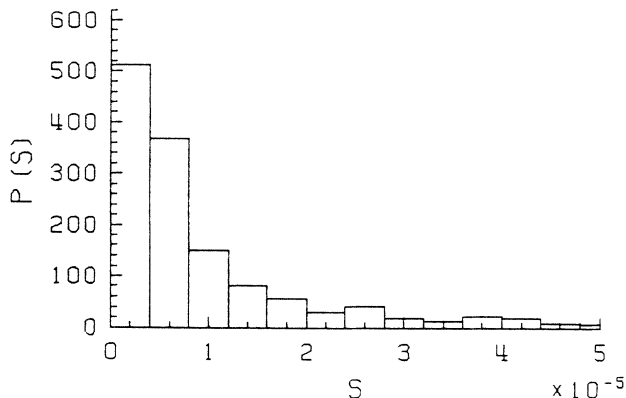


FIG. 3. Level distribution $P(S)$ for the on-site Fibonacci model ($v=1.8$), indicating the inverse power law behavior. (The system size is 1597.)

three groups according to the same rule, which continues to hold for the sub-subbands and so on. [Note that in Figs. 1(a) and 1(c) the straight lines of $G(n)$ are reminiscence of this branching rule]. As pointed out previously,^{9,13} the band structure in both models, the Harper model at $\lambda=2$ and the Fibonacci models, is self-similar. These facts remind us of the fractal nature¹⁶ of these systems in which the characteristic scale is absent and might be responsible for the IPL distribution, suggesting that self-similarity plays a crucial role similar to what translational symmetry does in ordinary crystals. The gross band structures are depicted in Fig. 4 for the Harper model. It is seen that the self-dual point $\lambda=2$ is a special point in this model.

We show the band measure defined by $\lim_{n \rightarrow \infty} M(n) = \lim_{n \rightarrow \infty} [2W - \sum_{k=1}^n G(k)] / 2W$, where $2W$ is the bandwidth for the Fibonacci on-site model in Fig. 5. It is readily seen that the band measure tends to vanish according to an inverse power law, implying that the band is a Cantor set which coincides with others.^{7,8} This fact holds for other values of v and also for the Fi-

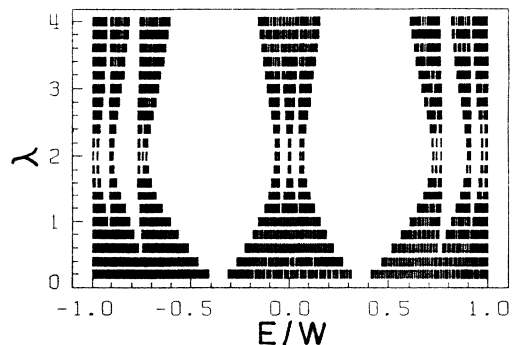


FIG. 4. Energy spectra normalized by the band width $2W$ of the Harper model for various potential strength λ . Gross band structures clearly indicate that the case $\lambda=2$ is special. (The system size is 1597.)

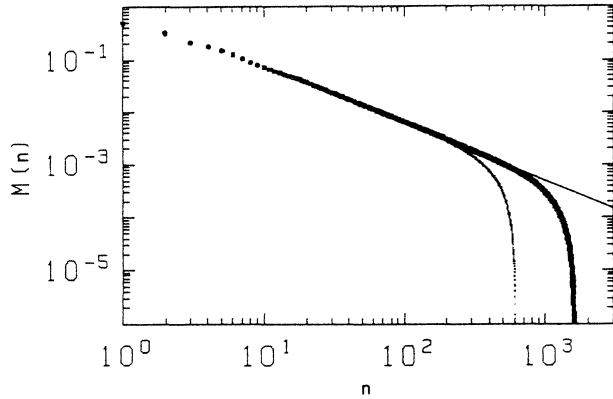


FIG. 5. $M(n)$ defined in the text for the on-site Fibonacci model ($\nu=1.8$). Large (small) dots correspond to the system size 1597 (610). Indicates that $M(n)$ tends to vanish according to the inverse power law (straight line).

bonacci transfer model and for the Harper model^{9,10} with $\lambda=2$.

In conclusion, we have found a distinctive change of the level distribution in the Harper model with incommensurate potentials, corresponding to the metal-insulator transition at the self-dual point $\lambda=2$ where the band structure is self-similar and the branching rule holds. In the localized region $\lambda > 2$ the level distribution is of Poisson type while at the critical point $\lambda=2$ it is of inverse-power-law type. We have also found the same level distribution in the Fibonacci models with quasiperiodic modulation. We suggest that the critical state intermediate between the localized and extended states is specified well by this novel type of inverse-power-law distribution.

We challenge some clever experimentalists to observe such a singular spectral distribution in the Fibonacci lattice, for example, synthesized recently by molecular beam epitaxy in GaAs-AlAs heterostructures¹⁵ or quasicrystals.¹⁴

¹For a recent review, see T. A. Brody *et al.*, *Rev. Mod. Phys.* **53**, 385 (1981).

²See the articles collected, in *Chaotic Behavior in Quantum Systems*, edited by G. Casati (Plenum, New York, 1985). For more recent references, see F. M. Izrailev, *Phys. Rev. Lett.* **56**, 541 (1986); T. Yukawa, *ibid.* **54**, 1883 (1985).

³D. R. Grempel *et al.*, *Phys. Rev. A* **29**, 269 (1985), and earlier papers therein. An excellent review article on this subject is given by R. E. Prange, D. R. Grempel, and S. Fishman, in Ref. 2. Some of the questions raised by them are resolved here.

⁴S. A. Molčanov, *Commun. Math. Phys.* **78**, 429 (1981).

⁵See for review, J. B. Sokoloff, *Phys. Rep.* **126**, 189 (1985).

⁶S. Aubry and G. Andre, *Ann. Israel Phys. Soc.* **3**, 134 (1980).

⁷M. Kohmoto *et al.*, *Phys. Rev. Lett.* **50**, 1870 (1983).

⁸S. Ostlund *et al.*, *Phys. Rev. Lett.* **50**, 1873 (1983).

⁹M. Kohmoto, *Phys. Rev. Lett.* **51**, 1198 (1983).

¹⁰S. Ostlund and R. Pandit, *Phys. Rev. B* **29**, 1394 (1984).

¹¹J. P. Lu *et al.*, *Phys. Rev. B* **33**, 4809 (1986).

¹²M. Kohmoto and J. R. Banavar, *Phys. Rev. B* **34**, 563 (1986).

¹³M. Fujita and K. Machida, *Solid State Commun.* **59**, 61 (1986). Also, see K. Machida and M. Fujita, *J. Phys. Soc. Jpn.* **55**, 1799 (1986) for the phonon problem.

¹⁴D. Shechtman *et al.*, *Rev. Lett.* **53**, 1951 (1984).

¹⁵R. Merlin *et al.*, *Phys. Rev. Lett.* **55**, 1768 (1985).

¹⁶B. B. Mandelbrot, *The Fractal Geometry of Nature* (Freeman, New York, 1983).

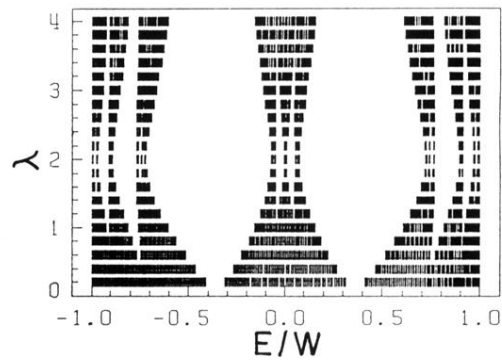


FIG. 4. Energy spectra normalized by the band width $2W$ of the Harper model for various potential strength λ . Gross band structures clearly indicate that the case $\lambda=2$ is special. (The system size is 1597.)